XXI Simposio CEA de Control Inteligente
24-26 de junio de 2026, Salamanca

Neuro-Fuzzy Modelling of a 50 MW Parabolic Trough Solar Loop

Ruiz-Moreno, S.[a], Fernández-Calatayud, F.[a,*], Gallego, A. J.[a], Maestre, J. M.[a], Escaño, J. M.[a]

[a]*Depto. de Ingeniería de Sistemas y Automática, Universidad de Sevilla, Camino de los Descubrimientos sin número, 41092, Sevilla, España*

To cite this article: Ruiz-Moreno, S., Fernández-Calatayud, F., Gallego, A. J., Maestre J. M., Escaño, J. M. 2020. Neuro-Fuzzy Modelling of a 50 MW Parabolic Trough Solar Loop. Revista Iberoamericana de Automática e Informática Industrial 00, 1-5. https://doi.org/10.4995/riai.2020.7133

Resumen

Este artículo presenta un modelo neuroborroso de un lazo de una planta de colectores cilindro-parabólicos de gran tamaño, implementado mediante *Adaptive Neuro-Fuzzy Inference System* (ANFIS). El enfoque propuesto sigue una filosofía de modelo de caja gris, combinando el conocimiento físico de la planta con un aprendizaje basado en datos para proporcionar un balance entre precisión, interpretabilidad y adaptabilidad. Debido a su eficiencia computacional y sus capacidades de adaptación, el modelo puede ser utilizado en tiempo real, por lo que es ideal para aplicaciones de gemelos digitales. Además, casos de uso potenciales incluyen aplicaciones en control predictivo, detección y diagnóstico de fallos en línea y tareas de monitorización para ciberseguridad. Los resultados obtenidos con datos de plantas reales demuestran la habilidad del modelo para reproducir con precisión la dinámica de la temperatura de salida de la planta en diferentes condiciones de operación, desde días soleados hasta nublados, por lo que resulta una herramienta fiable e interpretable para modelar plantas termosolares.

Palabras clave: Energia solar, Modelado de caja gris, Sistemas neuroborrosos, Modelado dinámico, Gemelos digitales.

Neuro-Fuzzy Modelling of a 50 MW Parabolic Trough Solar Loop

Abstract

This paper presents a Neuro-Fuzzy (NF) model of a loop of a large-scale Parabolic Trough Collector (PTC) plant implemented using an Adaptive Neuro-Fuzzy Inference System (ANFIS). The proposed approach follows a grey-box modeling philosophy, combining prior physical knowledge of the system with data-driven learning in order to achieve a proper balance between modeling accuracy, interpretability, and adaptability. Due to its computational efficiency and adaptive capabilities, the proposed NF model is suitable for real-time implementation, making it a promising candidate for digital twin applications in PTC plants. Potential use cases include predictive control-oriented modeling, online fault detection and diagnosis, and cybersecurity-related monitoring tasks. Performance results obtained using real plant data show that the proposed ANFIS model is able to accurately reproduce the outlet temperature dynamics under varying operating conditions, from sunny to partially cloudy and fully cloudy days, demonstrating its effectiveness as a reliable and interpretable modeling tool for solar thermal systems.

Keywords: Solar energy, Grey-box modelling, Neuro-fuzzy control, Dynamic modelling, Digital twins.

1. Introduction

Climate change and energy security have emerged as two of the major concerns of the present century (Suman, 2018). In this context, renewable energy sources are widely regarded as one of the most promising alternatives to fossil fuels in the near future, and significant research efforts have focused on commercially available technologies such as solar and wind energy (Sayed et al., 2023). Despite this growing interest, a large share of the electricity produced worldwide still relies on fossil fuels and other non-renewable energy sources (Heeckt and Kolaric, 2020). Among renewable options, solar energy is particularly attractive due to its abundance and global availability, as evidenced by the increasing number of solar power plants being deployed worldwide (Rakhshani et al., 2019).

*Autor para correspondencia: ffernandez11@us.es
Attribution-NonCommercial-ShareAlike 4.0 International (CC BY-NC-SA 4.0)

This work focuses on solar energy and, more specifically, on Concentrating Solar Power (CSP) technologies, which concentrate solar radiation to produce thermal energy for power generation and other applications such as solar cooling or desalination. CSP plants present several advantages, such as thermal inertia, mechanical inertia, and the capability of integrating thermal energy storage systems, which enhance their dispatchability. The main CSP technologies include Parabolic Trough Collectors (PTC), Linear Fresnel Reflectors (LFR), Solar Power Towers (SPT), and Parabolic Dish Systems (PDS). Among them, PTC technology stands out due to its technological maturity, proven large-scale deployment, and well-established operational experience. For these reasons, this work focuses on PTC plants.

However, large-scale PTC plants are highly nonlinear systems with complex dynamics, transient operations and an extensive spatial distribution. These characteristics make it particularly challenging to model them accurately and efficiently, which is important when the models are intended for advanced control strategies such as Model Predictive Control (MPC) (Camacho and Bordons, 2013). To address the computational burden associated with control and optimization, several approaches have been proposed in the literature. For instance, Masero et al. (2022) present a coalitional MPC approach based on market supply and demand to maximize thermal energy in PTC plants. Pataro et al. (2021) propose a mixed logical-dynamic model, linear in the state space, for controlling hybrid solar thermal plants while considering load demand variations. Frejo and Camacho (2020) introduce a distributed MPC algorithm to optimize the operation of solar field loops. Additionally, in a previous study by the authors (Ruiz-Moreno et al., 2025), neural networks were used to emulate a nonlinear MPC controller for electric power maximization, highlighting the potential of Artificial Intelligence (AI) techniques to drastically reduce computation times while learning from highly complex controllers.

An alternative research line focuses on obtaining faster models rather than replacing the control strategy itself (Schimperna et al., 2024). In this context, AI-based approaches have been widely adopted. Himour et al. (2023) linearize, at each sampling time, a neural network model of a PTC plant. In the work by Zaaoumi et al. (2021), an Artificial Neural Network (ANN) is proposed to estimate hourly electric production, outperforming two analytical models.

Despite their strong approximation capabilities, neural networks are often criticized for their black-box nature, which limits its interpretability. To overcome this limitation, fuzzy modeling offers a valuable alternative. The Adaptive Neuro-Fuzzy Inference System (ANFIS), introduced by Jang (1993), combines the learning capabilities and fast computation of neural networks with the interpretability of Fuzzy Inference Systems (FIS). This hybrid approach enables the integration of data-driven learning and expert knowledge through rule-based reasoning, facilitating a more transparent and adaptable modeling framework. Recent applications of ANFIS include the modeling of photovoltaic facilities (Chicaiza et al., 2025), as well as industrial automation tasks in the food industry (Marković et al., 2024). Regarding thermosolar applications, Machado et al. (2023) develop digital twin models of a Fresnel collector using both a phenomenological model based on Partial Differential Equations (PDE) and a data-driven ANFIS approach, while Rodríguez et al. (2023) combine neuro-fuzzy systems and recurrent neural networks for sensor fault detection and error prediction in a solar cooling plant. Specifically for PTC technology, Escaño et al. (2021) propose a nonlinear fuzzy MPC controller to reduce prediction time in an experimental PTC plant for outlet temperature regulation.

In this work, an ANFIS-based model is proposed for a large-scale PTC solar power plant equipped with a defocusing mechanism. Modeling such plants is particularly challenging due to the long collector loops, which increase thermal losses, and the presence of additional phenomena affecting energy capture, such as collector soiling (impacting optical efficiency) and defocusing efficiency. The proposed gray-box neuro-fuzzy methodology provides both interpretability and adaptability, allowing the model to be rapidly updated with new data and to accurately reflect the real behavior of the plant throughout its operational lifetime. The main contribution of this paper is the development and validation of a neuro-fuzzy model for a loop of a 50 MW PTC plant that explicitly accounts for defocusing strategies.

The remainder of this paper is organized as follows. Section 2 describes the plant, its main components, and the reference model and parameters. Section 3 presents the proposed modeling methodology. Simulation results are discussed in Section 4, and final conclusions are drawn in Section 5.

2. Plant Description

Table 1: Parameters descriptions

Symbol	Description	Units
t	Time	s
x	Space	m
ρ	Density	kg/m^3
C	Specific heat capacity	$JK^{-1}kg^{-1}$
A	Cross Sectional Area	m^2
T	Temperature	K,°C
$q(t)$	Oil flow rate	m^3s^{-1}
I	Solar irradiance	Wm^{-2}
n_o	Geometric efficiency	Unitless
K_{opt}	Optical efficiency	Unitless
G	Collector Aperture	m
T_a	Ambient Temperature	K,°C
T_f	Fluid Temperature	K,°C
T_m	Metal Temperature	K,°C
H_l	Global coefficient of thermal loss	$Wm^{-2}°C^{-1}$
H_t	Coefficient of heat transmission metal-fluid	$Wm^{-2}°C^{-1}$
L	Length of the pipe	m
δ	Declination	rad
ω	Angular displacement of the sun	rad
LH	Local time	Hours
S	Surface	m^2
θ_d	Defocusing angle	rad
ϕ	Latitude	rad

A PTC plant is a solar thermal power plant that uses parabolic reflectors to concentrate solar radiation onto a re-

ceiver tube, where a Heat Transfer Fluid (HTF), typically thermal oil, circulates. The concentrated solar rays heat the fluid, which is subsequently directed to a steam generator to produce electricity.

This work focuses on modelling focuses on modeling a single representative loop of a 50 MW solar trough plant. The loop has a a total length of 620 m and is composed of four collectors aligned in a north–south orientation, with an active section of 593 m and the parameters depicted in Table 1.

2.1. Distributed Parameter Model

The thermal behavior of the loop is modeled using a distributed-parameter formulation, governed by Equations 1 and 2 (Camacho et al., 2012), which describe the energy balance of both the receiver tube and the heat transfer fluid. It is assumed that the metallic wall exhibits a radially uniform temperature, and that the geometric properties of the reflector and receiver remain constant along the active sections of the loop. As a consequence, the local concentration ratio can be considered spatially invariant.

$$\rho_m C_m A_m \frac{\partial T_m}{\partial t} = I K_{opt} n_o G - H_l G(T_m - T_a) - L H_t (T_m - T_f) \quad (1)$$

$$\rho_f C_f A_f \frac{\partial T_f}{\partial t} + \rho_f C_f q \frac{\partial T_f}{\partial x} = L H_t (T_m - T_f) \quad (2)$$

The thermal loss coefficient and the internal convective heat transfer coefficient are computed using Equations 3 and 4, respectively.

$$H_l = 1.137 \cdot 10^{-8} (T_f - T_a)^3 - 3.235 \cdot 10^{-6} (T_f - T_a)^2 + 1.444 \cdot 10^{-4} (T_f - T_a) + 8.179 \cdot 10^{-2} - \frac{4.796}{(T_f - T_a)} \quad (3)$$

$$H_t = \left(\frac{q}{3600}\right)^{0.818} \left(-3.243 \cdot 10^{-4} T_f^3 + 2.442 \cdot 10^{-1} T_f^2 + 2.320 \cdot 10^{2} T_f + 2.532 \cdot 10^{4}\right) \quad (4)$$

Given the north–south orientation of the plant, the geometric efficiency is evaluated according to Equation 5 (Teleszewski et al., 2021).

$$n_o = \left((\sin(\phi)\sin(\delta_s) + \cos(\phi)\cos(\delta_s)\cos(\omega_s))^2 + \cos^2(\delta_s)\sin^2(\omega_s)\right)^{\frac{1}{2}} \quad (5)$$

The heat transfer fluid employed in the plant is Therminol VP-1. Its specific heat capacity and temperature-dependent density are described by Equations 7 and 6, respectively (Gallego et al., 2022).

$$\rho_f = -4.810 \cdot 10^{-4} T_f^2 - 8.110 \cdot 10^{-1} T_f + 9.537 \cdot 10^{2} \quad (6)$$

$$C_f = 1.561 \cdot 10^{-8} T_f^2 + 1.707 \cdot 10^{-1} T_f + 1.574 \cdot 10^{2} \quad (7)$$

Additionally, K_{opt} is modeled as 0.6290 for the first collector, 0.6790 for the second, 0.7290 for the third and 0.7190 for the fourth collector, G = 5.75 m, ρ_m = 7800 kg/m^3, C_m = 550 J/kg°C, A_f = 0.0036 m^2, A_m = 2.1677 × 10^{-4} m^2 and L = 0.2136 m.

For numerical integration, the loop is spatially discretized into 297 segments of 2.0625 m each. A temporal integration step of 0.25 s is adopted.

Finally, to guarantee safe and efficient operation, the maximum allowable temperature is limited to 400 °C. Moreover, the volumetric flow rate is restricted to the interval between 9 and 33 m^3/h in order to ensure adequate heat transfer and operational stability.

2.2. Concentrated Parameter Model

A simplified representation of the plant dynamics is provided by the concentrated-parameter approach, commonly referred to as the lumped-parameter model. This formulation captures the temporal evolution of the internal energy of the HTF and has been widely adopted in the literature. The resulting lumped-parameter model is mathematically described by Equation 8.

$$C_{loop} \frac{\partial T_{out}}{\partial t} = n_o K_{opt} S I - q P_{cp} (T_{out} - T_{in}) - H_l S (T_{mean} - T_a) \quad (8)$$

where $C_{loop} = L_{loop} \rho_{f,mean} C_{f,mean} A_f$ denotes the thermal capacity of the loop, $S = G L_{loop}$ is the effective aperture area, and $P_{cp} = \rho_m C_m$ corresponds to the thermal capacity of the pipe material. Moreover, T_{in} and T_{out} denote the inlet and outlet temperatures of the HTF and T_{mean} is the average temperature between inlet and outlet.

2.3. Defocus Mechanism

The plant features a defocusing algorithm to reduce the collector efficiency when some maximum temperature limits are exceeded or the system is under power constraints, ensuring safe plant operation. This mechanism steers the collectors away from their focal point to reduce the incident radiation on the receiver and is widely adopted in commercial plants. The strategy adopted relies on a three-state logic, illustrated in Figure 1.

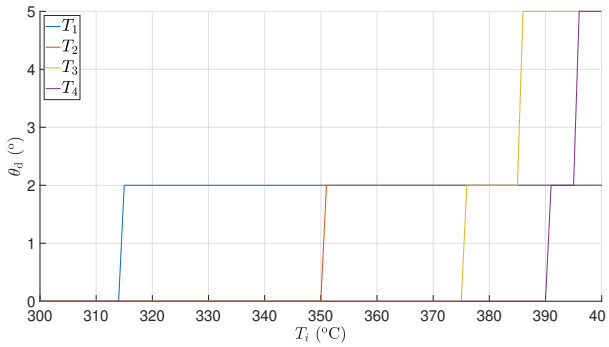


Figure 1: Defocusing strategy. T_i is the temperature at the center of collector i and θ_d is the defocusing angle.Only collectors 3 and 4 can reach the three states.

In this scheme, state 0 corresponds to a defocusing angle of $\theta_d = 0°$, state 1 to $\theta_d = 2°$, and state 2 to $\theta_d = 5°$. Transitions between states depend on the measured temperature at the center of each collector. Collectors 1 and 2 operate only in states 0 and 1, whereas collectors 3 and 4 can operate in all three states.

The defocusing angle–efficiency relationship is defined by the curve depicted in Figure 2.

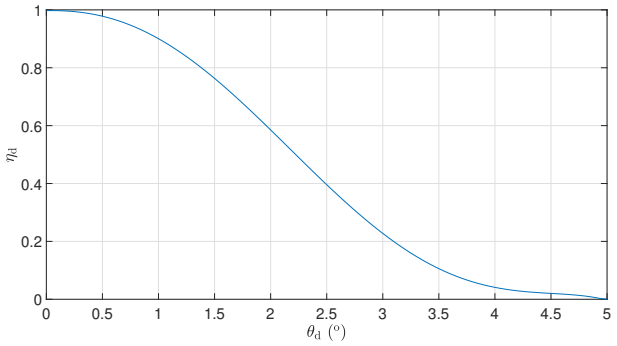


Figure 2: Efficiency curve as a function of the defocusing angle

2.4. Plant Controller

To regulate the plant operation, a feedforward controller Camacho et al. (2012) is employed to track a desired outlet temperature T_{ref} by manipulating the volumetric flow rate in the loop and reject disturbances. The controller operates with a sampling time of 30 s and is based on a steady-state lumped-parameter model. The control law is given by Equation 9.

$$q = \frac{n_{\mathrm{o}} K_{\mathrm{opt}} S\, I - H_{\mathrm{l}} S\,(T_{\mathrm{mean}} - T_{\mathrm{a}})}{P_{\mathrm{cp}}(T_{\mathrm{ref}} - T_{\mathrm{in}})} \tag{9}$$

The controller is designed to maintain the flow rate within the operating range of 9 m^3/h to 33 m^3/h, ensuring that the outlet temperature does not exceed 400 °C. Lastly, the controller assumes a K_{opt} of 0.64881.

3. Methodology

The ANFIS system (Karaboga and Kaya, 2019) emerges from the combination of ANNs and FIS to exploit the learning capabilities of data-driven models while preserving the interpretability of fuzzy rule-based structures. Its main purpose is to optimize membership function parameters through supervised learning, enabling the FIS to accurately map input-output data pairs. In the Takagi–Sugeno formulation adopted in ANFIS, the inference structure relies on functional consequents rather than weighted connections, allowing for efficient signal propagation and fast computation (Takagi and Sugeno, 1985).

Structurally, the model is organized into five distinct layers. The fuzzification and defuzzification layers employ adaptive nodes to enable parameter tuning, whereas the intermediate layers consist of fixed nodes. This architecture is particularly effective when traditional mathematical modeling is hindered by system complexity or inherent uncertainty. In this study, ANFIS is employed to capture the temperature dynamics of the PTC plant, with the fuzzy rules generated using the Fuzzy C-Means (FCM) clustering algorithm. FCM was selected due to its ability to automatically identify clusters while allowing partial membership.

To capture the dynamic behavior of the solar field, the ANFIS input vector was constructed by combining key physical variables with autoregressive terms, based on prior expert knowledge of the system. The selected features include the inlet temperature $T_{\mathrm{in}}(k)$, the volumetric flow rate $q(k)$, and the modified irradiance reaching the receiver tube, expressed as $I(k)\, n_{\mathrm{o}}(k)\, K_{\mathrm{opt}}^{\mathrm{av}}$, where $K_{\mathrm{opt}}^{\mathrm{av}} = 0.6921$ represents the average optical efficiency of the field (with value 0.6921). To account for thermal inertia and transient effects, delayed values of the outlet temperature, namely $T_{\mathrm{out}}(k-1)$ and $T_{\mathrm{out}}(k-2)$, were incorporated into the model. In addition, the average defocusing angle was included to reflect efficiency variations due to operational constraints. Finally, a normalized non-linear interaction term, defined as $q\, T_{\mathrm{out}}(k-1)/30$, was introduced.

4. Results

This section presents the results obtained after training the proposed ANFIS model. The dataset was generated from 60 simulations using real solar irradiance and inlet temperature profiles corresponding to sunny, partially cloudy, and cloudy days, assuming fixed optical efficiencies. In half of the simulations, the system was controlled using the feedforward controller described in Section 2.4, with outlet temperature references randomly updated every hour and maximum step changes of ±10°C. In the remaining simulations, the volumetric flow rate was randomly updated every 30 minutes with maximum step changes of ±0.5 m^3/h. The dataset sampling time was 10 s. All simulations and training procedures were carried out in MATLAB® R2024b using the Fuzzy Logic Toolbox on an Intel® Core™ i7-9700F CPU at 3.00 GHz with 16 GB of RAM.

The dataset was randomized and divided into training (80%), validation (10%), and test (10%) subsets. The FIS was generated using Fuzzy C-Means (FCM) clustering and trained for 125 epochs. Table 2 reports the Root Mean Square Errors (RMSEs) and mean percentage errors of the estimated outputs in close loop with respect to the actual temperature for models with 2, 4, 6, and 8 clusters.

Table 2: Prediction errors for different size models

Clusters	RMSE			Mean percentage error (%)			Training time (s)
	Training	Validation	Test	Training	Validation	Test	
2	0.96652	0.96518	1.0115	0.17615	0.17473	0.1762	85.3923
4	0.7689	0.7485	0.7601	0.1434	0.1428	0.1423	167.8297
6	0.73954	0.74187	0.73521	0.13786	0.13869	0.1385	266.7165
8	0.70903	0.7147	0.69353	0.12807	0.12848	0.12778	474.5305

As shown in Table 2, the average prediction errors decrease as the number of clusters increases, at the cost of higher training times. The model with 8 clusters was selected as a trade-off between accuracy, training time, and interpretability.

After training and selecting the best-performing FIS, three additional simulations were conducted using previously unseen irradiance and ambient temperature profiles to evaluate the model in closed-loop operation. Table 3 presents the RMSEs, mean percentage errors, and average computation times for sunny, partially cloudy, and cloudy days and the overall average.

Table 3: Closed-loop prediction errors

Day	RMSE	Perc. error (%)	Comput. time
Sunny	0.6634	0.1271	$2.7050{\cdot}10^{-4}$
Partially cloudy	0.6781	0.1265	$2.6793{\cdot}10^{-4}$
Cloudy	0.8406	0.1370	$2.7062{\cdot}10^{-4}$
All	0.69353	0.12778	$2.7005{\cdot}10^{-4}$

In all cases, the prediction errors remain low and consistent across different operating conditions. Slightly higher errors are observed during the cloudy day, where the system dynamics are more complex due to rapid irradiance variations.

Figure 3 shows the modified irradiance, flow rate, and defocusing angles for the sunny-day experiment. Due to the high irradiance levels, the flow rate becomes saturated and the collectors remain defocused for most of the simulation, which increases the difficulty of accurately modeling the system dynamics.

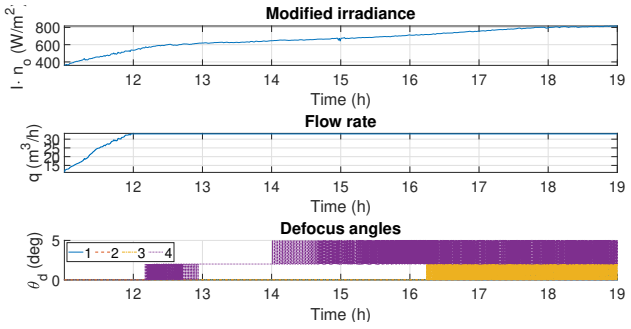


Figure 3: Simulation conditions of the experiment with the sunny day.

The corresponding modeling results are presented in Figure 4, where prediction errors remain below 3°C for most of the simulation, showing high steady-state tracking accuracy.

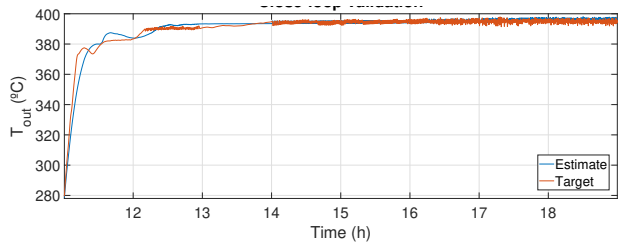


Figure 4: Modelling results of the experiment with the sunny day.

The simulation conditions for the partially cloudy day are shown in Figure 5, where a medium-sized cloud appears around 15:00, causing a sudden drop in the solar irradiance profile.

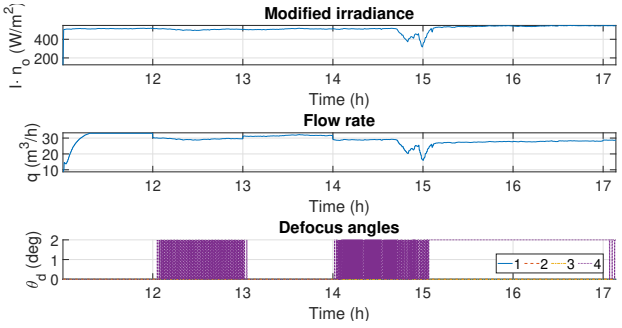


Figure 5: Simulation conditions of the experiment with the partially cloudy day.

The corresponding estimation results are depicted in Figure 6, demonstrating that the model absorbs the cloud disturbance rapidly and maintains a good steady-state performance.

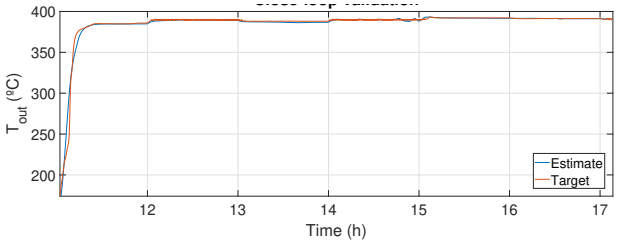


Figure 6: Modelling results of the expertiment with the partially cloudy day.

Finally, Figure 7 presents the simulation conditions for the cloudy day, characterized by highly dynamic solar fluctuations where defocusing angles have a reduced impact due to lower irradiance levels.

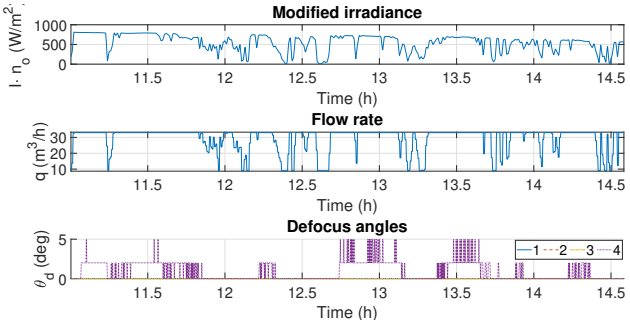


Figure 7: Simulation conditions of the expertiment with the cloudy day.

The modeling results are shown in Figure 8. Even under these highly dynamic conditions, the ANFIS model accurately approximates the outlet temperature and successfully captures the system dynamics.

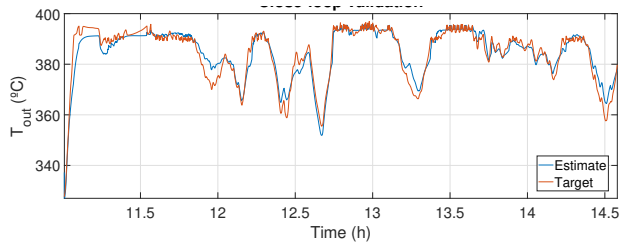


Figure 8: Modelling results of the expertiment with the cloudy day.

5. Conclusions

The results presented in this work demonstrate the suitability of ANFIS-based modeling for capturing the dynamic thermal behavior of large-scale parabolic trough collector (PTC) plants with defocusing mechanism under varying operating conditions. By combining expert-driven variable selection with data-driven learning, the proposed approach achieves a flexible representation of the nonlinear relationships governing the outlet temperature of the solar field. Moreover, the integration of physical variables with autoregressive terms proved essential to account for thermal inertia and transient effects, which are characteristic of large-scale solar thermal systems.

Unlike purely black-box models, the ANFIS structure preserves a degree of transparency while maintaining sufficient modeling accuracy, making it particularly attractive for applications where uncertainty, nonlinearity, and limited physical modeling capabilities coexist.

Overall, the proposed methodology provides a robust and interpretable framework for data-driven modeling of PTC plant temperature dynamics and constitutes a promising basis for future developments in control, fault detection, or cybersecurity applications.

Future work will focus on extending the proposed ANFIS framework to improve robustness and adapt membership function parameters to cope with long-term performance degradation and aging effects in the solar field. Finally, the integration of the proposed model into control-oriented applications, such as MPC or fault detection schemes, will be assessed in order to evaluate its practical applicability in real plant operation.

Acknowledgments.

This project was supported by the Spanish Ministerio de Ciencia, Innovación y Universidades under the FPI grant (No. INV-PRE-2024-I-034) and the project Control Coalicional para la Optimización de Sistemas Ciberfísicos: Ronda 3 (No. PID2023-152876OB-I00).

Disclosure of Interests.

The authors have no competing interests to declare that are relevant to the content of this article.

References

Camacho, E. F., Berenguel, M., Rubio, F. R., Martinez, D., 1 2012. Control of solar energy systems. Springer-Verlag.

Camacho, E. F., Bordons, C., 2013. Model predictive control. Springer Science & Business Media.

Chicaiza, W. D., Topa, A. O., Sánchez, A. J., Escaño, J. M., Álvarez, J. D., 2025. Model design for photovoltaic facilities based on fuzzy neural network as core of its digital twin. Energy Conversion and Management 342, 120001.

Escaño, J. M., Gallego, A. J., Sánchez, A. J., Yebra, L. J., Camacho, E. F., 2021. Nonlinear fuzzy model predictive control of the {TCP-100} parabolic trough plant. In: 19th World Congress of the International Fuzzy Systems Association (IFSA), 12th Conference of the European Society for Fuzzy Logic and Technology (EUSFLAT), and 11th International Summer School on Aggregation Operators (AGOP). pp. 235–241.
DOI: https://doi.org/10.2991/asum.k.210827.032

Frejo, J. R. D., Camacho, E. F., 7 2020. Centralized and distributed model predictive control for the maximization of the thermal power of solar parabolic-trough plants. Solar Energy 204, 190–199.
DOI: 10.1016/j.solener.2020.04.033

Gallego, A. J., Macías, M., de Castilla, F., Sánchez, A. J., Camacho, E. F., 2022. Model predictive control of the Mojave solar trough plants. Control Engineering Practice 123, 105140.

Heeckt, C., Kolaric, S., 2020. Urban sustainability in europe: What is driving cities' environmental changes. Tech. rep., Tech. rep., European Environment Agency. URL: https://www. eea. europa. eu ....

Himour, Y., Tadjine, M., Boucherit, M. S., 2023. Nonlinear and infinite gain scheduling neural predictive control of the outlet temperature in a parabolic trough solar field: A comparative study. Engineering Applications of Artificial Intelligence 126, 106862.

Jang, J.-S., 1993. Anfis: adaptive-network-based fuzzy inference system. IEEE transactions on systems, man, and cybernetics 23 (3), 665–685.

Karaboga, D., Kaya, E., 2019. Adaptive network based fuzzy inference system (anfis) training approaches: a comprehensive survey. Artificial Intelligence Review 52, 2263–2293.

Machado, D. O., Chicaiza, W. D., Escaño, J. M., Gallego, A. J., de Andrade, G. A., Normey-Rico, J. E., Bordons, C., Camacho, E. F., 2023. Digital twin of a fresnel solar collector for solar cooling. Appl. Energy 339, 120944.

Marković, N., Ćirić, I., Ćojbašić E Ivačko, et al., 2024. Anfis based explainable ai approach for industrial automation in the food industry. In: Proceedings of the ICIST.

Masero, E., Maestre, J. M., Camacho, E. F., 2022. Market-based clustering of model predictive controllers for maximizing collected energy by parabolic-trough solar collector fields. Applied Energy 306, 117936.
DOI: https://doi.org/10.1016/j.apenergy.2021.117936

Pataro, I. M. L., Gil, J. D., da Costa, M. V. A., Guzmán, J. L., Berenguel, M., 2021. A nonlinear control approach for hybrid solar thermal plants based on operational conditions. Renewable Energy.
URL: https://www.sciencedirect.com/science/article/pii/S0960148121015159
DOI: https://doi.org/10.1016/j.renene.2021.10.057

Rakhshani, E., Rouzbehi, K., Sánchez, A. J., Tobar, A. C., Pouresmaeil, E., 2019. Integration of large scale {PV}-based generation into power systems: A survey. Energies 12, 1425.

Rodríguez, F., Chicaiza, W. D., Sánchez, A., Escaño, J. M., 2023. Updating digital twins: Methodology for data accuracy quality control using machine learning techniques. Computers in Industry 151, 103958.

Ruiz-Moreno, S., Gallego, A., Frejo, J., Camacho, E., 2025. Electric power optimization in solar trough plants with deep learning-based model predictive control.

Sayed, E. T., Olabi, A. G., Alami, A. H., Radwan, A., Mdallal, A., Rezk, A., Abdelkareem, M. A., 2023. Renewable energy and energy storage systems. Energies 16, 1415.

Schimperna, I., Galuppini, G., Magni, L., 2024. Recurrent neural network based mpc for systems with input and incremental input constraints. IEEE Control Systems Letters.

Suman, S., 2018. Hybrid nuclear-renewable energy systems: A review. Journal of Cleaner Production 181, 166–177.
DOI: https://doi.org/10.1016/j.jclepro.2018.01.262

Takagi, T., Sugeno, M., 1985. Fuzzy identification of systems and its applications to modeling and control. IEEE Transactions on Systems, Man, and Cybernetics SMC-15 (1), 116–132.
DOI: 10.1109/TSMC.1985.6313399

Teleszewski, T. J., Żukowski, M., Krawczyk, D. A., Rodero, A., 2021. Analysis of the applicability of the parabolic trough solar thermal power plants in the locations with a temperate climate. Energies 14, 3003.

Zaaoumi, A., Bah, A., Ciocan, M., Sebastian, P., Balan, M. C., Mechaqrane, A., Alaoui, M., 2021. Estimation of the energy production of a parabolic trough solar thermal power plant using analytical and artificial neural networks models. Renewable Energy 170, 620–638.
URL: https://www.sciencedirect.com/science/article/pii/S0960148121001361
DOI: https://doi.org/10.1016/j.renene.2021.01.129